Quadruple Spherical Harmonics Approximation for Radiative Transfer in Two-Dimensional Rectangular Enclosures

R. K. Iyer* and M. P. Mengüc†
University of Kentucky, Lexington, Kentucky

A hybrid model is developed for the solution of the radiative transfer equation (RTE) in two-dimensional rectangular enclosures by combining a four-flux method with the first-order spherical harmonics approximation. The governing equations of the model are comprised of 12 first-order partial differential equations. In the formulation, a delta-Eddington phase function is employed, and emitting and diffusely reflecting boundaries are considered. Numerical solutions of the equations are obtained using a software package DISPL2 and the results are compared with those available in the literature. In general, very good agreement is observed between the heat flux predictions of the model and the exact results.

Nomenclature

f = delta-Eddington phase function parameter, Eq. (23)
g = delta-Eddington phase function parameter, Eq. (23)
h = boundary intensities
x = Cartesian coordinate; normalized optical thickness, Eq. (26)
z = Cartesian coordinate; normalized optical thickness, Eq. (26)
A_i = coefficients of intensity, Eqs. (4)
B_i = coefficients of intensity, Eqs. (6)
C_i = coefficients of intensity, Eqs. (7)
D_i = coefficients of intensity, Eqs. (8)
E_i = coefficients of intensity, Eqs. (9)
K_i = sum of moments, Eq. (29)
M = intensity in positive x direction
M_i = moments of intensity, Eqs. (10–12)
M_{ij} = double moments of intensity, Eqs. (16–18)
N = intensity in negative x direction
N_{ij} = double moments of intensity
P_l^m = associated Legendre polynomials, Eq. (2b)
P_j = coefficients of Eqs. (34–39); see the appendix
q = radiative heat flux, Eqs. (46–49)
S = source term, right-hand side of Eq. (22)
T = temperature
β = extinction coefficient (m^{-1})
δ = Kronecker delta function
ϵ = emissivity
θ = zenith angle
μ = direction cosine in z direction, $\cos\theta$
ξ = direction cosine in x direction, $\sin\theta\cos\phi$
ρ = reflectivity
τ = optical thickness
ϕ = azimuthal angle
ω = single scattering albedo
Θ = scattering angle
Φ = scattering phase function
Ω = solid angle

Subscripts and Superscripts

0 = normalized quantities
b = blackbody emission
w = boundary surface
1 = ξ direction cosine
2 = η direction cosine
3 = μ direction cosine
+ = upper hemisphere
− = lower hemisphere

Introduction

RADIATION heat transfer becomes increasingly important because of its wide applications in high-temperature practical systems like furnaces, combustors, and engines.[1] The RTE (radiative transfer equation) is an integrodifferential equation in terms of radiation intensity that has spectral, spatial, and angular dependency. Radiation intensity also has a functional dependence on the temperature distribution, as well as on the absorbing, emitting, and scattering properties of the medium. Several different solution techniques for the RTE have been developed over the years, some of which have been exact, but many have been approximate. Most models for the RTE are limited in scope. As a result, no single model can be used for all classes of problems. In order to take advantage of the desirable features of the different models, two or more techniques can be coupled together to develop hybrid radiative transfer models. Detailed reviews of these techniques are available in the literature.[1-3] Here, we will cite only the most relevant works.

Krook[4] combined flux and moment methods to derive the adapted moment method, where the intensity is defined for two regions, and in each region it is expressed as a sum of its moments. This approach yielded better results than the moment method of the same order, especially at the boundaries. A similar method using the first-order spherical harmonics approximation and a two-flux method was developed by Yvon[5] for a one-dimensional plane-parallel medium. This method, which was used by Ziering and Schiff[6] for a plane geometry with isotropic scattering, can be called a double spherical harmonics approximation. Schiff and Ziering[7] extended this technique to a two-dimensional geometry using four divisions of the spherical space and employed an eigenvalue solution to the problem. The double spherical harmonics method has also been used by Le Sage[8] to solve the one-dimensional RTE.

Received Jan. 4, 1988; revision received May 9, 1988.

*Research Assistant, Department of Mechanical Engineering.
†Associate Professor, Department of Mechanical Engineering.

A half-range method moment analysis was formulated by Özisik et al.[9] for a spherically symmetric enclosure. The method is an extension of Sherman's moment formulation for a plane-parallel geometry.[10] Selcuk and Siddall[11] formulated the RTE using the P_1 approximation, and then they reduced it to a two-flux form using an averaging procedure. Wan et al.[12] used the double spherical harmonics method to formulate the RTE in a slab with anisotropic scattering. An exponential form of the solution was assumed and solved. Another model was suggested by Wilson and Sen[13] in which the radiation field in a plane-parallel medium was divided into four subregions. Harshvardhan et al.[14] modeled the transport of infrared radiation in cuboidal clouds. Using a P_1 approximation for the vertical direction, they assumed the intensities to be evaluated at the values of the first Gaussian quadrature points. Recently, Mengüc and Iyer[15] formulated and solved a double spherical harmonics (DP_1) approximation in one-dimensional, absorbing, emitting, and anisotropically scattering media. Instead of following an eigenvalue-eigenvector solution approach to the problem, they obtained first-order differential equations in terms of half-space moments, which can be solved easily and quickly using available solution algorithms. Comparison of the DP_1 approximation predictions with the benchmark results showed excellent agreement. They also gave the formulation of the octuple spherical harmonics (OP_1) approximation for two-dimensional, axisymmetric cylindrical enclosures.

Results from one-dimensional studies show that hybrid models are quite accurate, very effective in many cases, and can be easily extended to multidimensional geometries. Selection of the right combination of the various methods is very important in determining the usefulness of a hybrid model. In this study, an approximate hybrid model is developed to solve the RTE in a two-dimensional rectangular enclosure containing an inhomogeneous, absorbing, emitting, and anisotropically scattering medium and bounded by emitting and reflecting walls. In the analysis, a four-flux model is used with the P_1 approximation and the higher-order moments are employed explicitly to apply the closure conditions. The technique, which is called the quadruple spherical harmonics (QP_1) approximation, is simple in formulation; however, it is slightly tedious in derivation because of the algebra involved. The formulation is based mainly on the idea of Schiff and Ziering,[6,7] although the present model differs from their technique in that they used an eigenvalue method for solving the differential equations, which cannot be extended to inhomogeneous media.

Analysis

Radiation Intensity

The radiation intensity can be expressed in terms of spherical harmonics in order to separate the angular and spatial variations and is written as[16]

$$I(\bar{r}, \hat{\Omega}) = \sum_{l=0}^{\infty} \sum_{m=-l}^{l} A_l^m(\bar{r}) Y_l^m(\hat{\Omega}) \tag{1}$$

where

$$Y_l^m(\hat{\Omega}) = K_l^m(\mu) e^{im\phi} \tag{2a}$$

are the spherical harmonics and

$$K_l^m(\mu) = \left[\frac{2l+1}{4\pi} \frac{(l-|m|)!}{(l+|m|)!}\right]^{1/2} (-1)^{(m+|m|)/2} P_l^{|m|}(\mu) \tag{2b}$$

Here, P_l^m are the associated Legendre polynomials and they are related to the Legendre polynomials. If the summation in Eq. (1) is done to infinity, we get the exact expression for the intensity. For the P_1 approximation, we have $l = 1$ as the upper limit. We can thus write the expression for the intensity as

$$I(\bar{r}, \hat{\Omega}) = A_0^0 Y_0^0 + A_1^0 Y_1^0 + A_1^1 Y_1^1 + A_1^{-1} Y_1^{-1} \tag{3}$$

We now substitute for the spherical harmonics expression Eq. (2a) in Eq. (3) and use the relations

$$P_0(\mu) = 1, \qquad P_1(\mu) = \mu$$

to obtain

$$K_0^0 = \left(\frac{1}{4\pi}\right)^{1/2}, \qquad K_1^0 = \left(\frac{3}{4\pi}\right)^{1/2} \mu$$

$$K_1^1 = \left(\frac{3}{8\pi}\right)^{1/2} \sin\theta, \qquad K_1^{-1} = -\left(\frac{3}{8\pi}\right)^{1/2} \sin\theta$$

Then, the radiation intensity becomes

$$I(\bar{r}, \hat{\Omega}) = A_0 + A_1 \xi + A_2 \mu + A_3 \eta \tag{4}$$

where

$$A_0 = A_0^0 \left(\frac{1}{4\pi}\right)^{1/2}, \qquad A_1 = \left(A_1^1 - A_1^{-1}\right)\left(\frac{3}{4\pi}\right)^{1/2}$$

$$A_2 = A_1^0 \left(\frac{3}{4\pi}\right)^{1/2}, \qquad A_3 = \left(A_1^1 + A_1^{-1}\right)\left(\frac{3}{4\pi}\right)^{1/2} \tag{5}$$

Because we are interested in solving the RTE in rectangular enclosures, we need to consider only two orthogonal coordinates. A schematic of the rectangular geometry is shown in Fig. 1. We choose x and z directions, with direction cosines ξ and μ, respectively. Thus, we set the coefficient of η as zero since we have no variation in the y direction.

We now introduce the quadruple spherical harmonics approximation. The intensity distribution is divided into four

Table 1 Angular division of radiation intensity

Domain	θ	ϕ	I	$d\Omega$
1	$0/\frac{\pi}{2}$	$-\frac{\pi}{2}/\frac{\pi}{2}$	M^+	Ω_1
2	$\frac{\pi}{2}/\pi$	$-\frac{\pi}{2}/\frac{\pi}{2}$	M^-	Ω_2
3	$0/\frac{\pi}{2}$	$\frac{\pi}{2}/\frac{3\pi}{2}$	N^+	Ω_3
4	$\frac{\pi}{2}/\pi$	$\frac{\pi}{2}/\frac{3\pi}{2}$	N^-	Ω_4

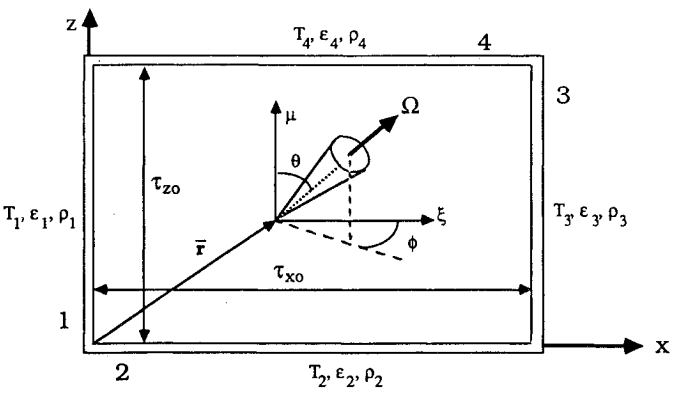

Fig. 1 Schematic of the two-dimensional rectangular geometry.

components based on the spherical domain, and the limits of each subdomain are shown in Table 1. A graphical representation is also shown in Fig. 2. The intensities in these four domains can be written as

$$M^+ = B_0 + B_1\xi + B_2\mu \tag{6}$$

$$M^- = C_0 + C_1\xi + C_2\mu \tag{7}$$

$$N^+ = D_0 + D_1\xi + D_2\mu \tag{8}$$

$$N^- = E_0 + E_1\xi + E_2\mu \tag{9}$$

The B, C, D, and E coefficients can be determined by integrating the intensities in their respective domains after multiplying by 1, ξ, and μ. This will yield three linear equations in each domain in terms of the moments of intensity, $M_0^{\pm}$, $M_1^{\pm}$, $M_3^{\pm}$, $N_0^{\pm}$, $N_1^{\pm}$, $N_3^{\pm}$. Following this procedure, we obtain

$$M_0^+ = \int_{\theta=0}^{\pi/2}\int_{\phi=-(\pi/2)}^{\pi/2} M^+ \, d\Omega = \pi B_0 + \frac{\pi}{2} B_1 + \frac{\pi}{2} B_2 \tag{10}$$

$$M_1^+ = \int_{\theta=0}^{\pi/2}\int_{\phi=-(\pi/2)}^{\pi/2} \xi M^+ \, d\Omega = \frac{\pi}{2} B_0 + \frac{\pi}{3} B_1 + \frac{2}{3} B_2 \tag{11}$$

$$M_3^+ = \int_{\theta=0}^{\pi/2}\int_{\phi=-(\pi/2)}^{\pi/2} \mu M^+ \, d\Omega = \frac{\pi}{2} B_0 + \frac{2}{3} B_1 + \frac{\pi}{3} B_2 \tag{12}$$

We solve Eqs. (10–12) for B_0, B_1, and B_2 using Cramer's rule, which yields

$$B_0 = a_1 M_0^+ + a_2 M_1^+ + a_2 M_3^+ \tag{13}$$

$$B_1 = a_2 M_0^+ + a_3 M_1^+ + a_4 M_3^+ \tag{14}$$

$$B_2 = a_2 M_0^+ + a_4 M_1^+ + a_3 M_3^+ \tag{15}$$

To obtain the coefficients in the other three domains, we use Eqs. (13–15), but replace M_1^+ by M_1^-, N_1^+, or N_1^-; replace B with C, D, or E; and use the appropriate signs as shown in Table 2.

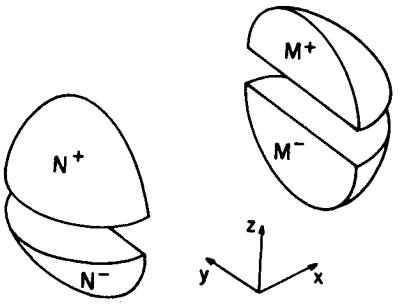

Fig. 2 Schematic of the radiation intensity distribution for the quadruple spherical harmonics (QP_1) approximation.

We next obtain the double moments of intensity by multiplying Eqs. (6–9) by ξ^2, μ^2, and $\xi\mu$ in turn and by integrating over the appropriate domain

$$M_{11}^+ = \int_{\theta=0}^{\pi/2}\int_{\phi=-(\pi/2)}^{\pi/2} \xi^2 M^+ \, d\Omega = \frac{\pi}{3} B_0 + \frac{\pi}{4} B_1 + \frac{\pi}{8} B_2 \tag{16}$$

$$M_{33}^+ = \int_{\theta=0}^{\pi/2}\int_{\phi=-(\pi/2)}^{\pi/2} \mu^2 M^+ \, d\Omega = \frac{\pi}{3} B_0 + \frac{\pi}{8} B_1 + \frac{\pi}{4} B_2 \tag{17}$$

$$M_{13}^+ = \int_{\theta=0}^{\pi/2}\int_{\phi=\pi/2}^{\pi/2} \xi\mu M^+ \, d\Omega = \frac{2}{3} B_0 + \frac{\pi}{8} B_1 + \frac{\pi}{8} B_2 \tag{18}$$

We now substitute Eqs. (13–15) for B_0, B_1, and B_2 in Eqs. (16–18) to obtain the double moments in terms of the zeroth and first-order moments

$$M_{11}^+ = P_1 M_0^+ + P_2 M_1^+ + P_3 M_3^+ \tag{19}$$

$$M_{33}^+ = P_1 M_0^+ + P_3 M_1^+ + P_2 M_3^+ \tag{20}$$

$$M_{13}^+ = P_4 M_0^+ + P_5 M_1^+ + P_5 M_3^+ \tag{21}$$

The P constants are listed in the Appendix. Similarly, we obtain the double moments in terms of the zeroth and first-order moments for the other domains from Eqs. (19–21). The necessary sign changes are to be introduced from Table 3. The technique of expressing higher-order moments in terms of lower-order moments is basically the application of the closure condition in the spherical harmonics approximation. Now, we can use the relations obtained to solve the radiative transfer equation.

Radiative Transfer Equation

The RTE for two-dimensional Cartesian geometry is written as[1]

$$\left[\frac{1}{\beta}\left(\xi\frac{\partial}{\partial x} + \mu\frac{\partial}{\partial z}\right) + 1\right] I(x, z, \theta, \phi) = (1-\omega) I_b\left[T(x, z)\right] + \frac{\omega}{4\pi}\int_{\phi'=0}^{2\pi}\int_{\theta'=0}^{\pi} I(x, z, \theta', \phi')\Phi(\theta, \phi, \theta', \phi') \, d\Omega' \tag{22}$$

The scattering phase function is approximated by the delta-Eddington phase function

$$\Phi(\cos\Theta) = 4\pi f\delta(1-\cos\Theta) + (1-f)(1+3g\cos\Theta) \tag{23}$$

This phase function is appropriate and very useful for modeling acutely anisotropic scattering,[17] and recently was discussed in detail by Crosbie and Davidson.[18] If $f = 0$, then the phase function reduces to the linearly anisotropic phase function provided that $a_1 = 3g$, where a_1 is the first coefficient of the Legendre polynomial expansion of the phase function. Substituting Eq. (23) into the last term of Eq. (22) and using

Table 2 Sign convention for the B, C, D, and E coefficients, Eqs. (13–15)

i	B_i	C_i	D_i	E_i
0	+ + +	+ + −	+ − +	+ − −
1	+ + +	+ + −	− + −	− + +
2	+ + +	− − +	+ − +	− + +

Table 3 Sign convention for the second-order moments, Eqs. (19–21)

ij	M_{ij}^+	M_{ij}^-	N_{ij}^+	N_{ij}^-
11	+ + +	+ + −	+ − +	+ − −
33	+ + +	+ + −	+ − +	+ − −
13	+ + +	− − +	− + −	+ − −

the moments of intensity, we obtain

$$\int_{\phi'=0}^{2\pi}\int_{\theta'=0}^{\pi} I(x, z, \theta', \phi')\Phi(\theta, \phi, \theta', \phi')\,d\Omega'$$
$$= 4\pi f I + (1-f)\left[(M_0^+ + M_0^- + N_0^+ + N_0^-)\right.$$
$$+ 3g(M_1^+ + M_1^- + N_1^+ + N_1^-)\xi$$
$$\left.+ 3g(M_3^+ + M_3^- + N_3^+ + N_3^-)\mu\right] \quad (24)$$

Because we are considering a two-dimensional problem, $M_2^{\pm}$, and $N_2^{\pm}$ are set equal to zero. Now, we define the optical thicknesses in the x and z directions as

$$\tau_x = \beta(1-\omega)x, \qquad \tau_z = \beta(1-\omega)z \quad (25)$$

and normalize them by τ_{x0} and τ_{z0}, such as

$$x' = \frac{\tau_x}{\tau_{x0}}, \qquad z' = \frac{\tau_z}{\tau_{z0}} \quad (26)$$

For the sake of clarity, we will use x and z, instead of x' and z', in the rest of the paper; however, it is understood that x and z are dimensionless. If we substitute Eq. (24) into Eq. (22), divide it by $(1-\omega f)$, and use the normalized optical thickness expressions, we obtain the RTE as

$$\left[\left(\frac{\xi}{\tau_{x0}}\frac{\partial}{\partial x} + \frac{\mu}{\tau_{z0}}\frac{\partial}{\partial z}\right) + 1\right] I(x, z, \theta, \phi)$$
$$= I_{b0}\left[T(x, z)\right] + \frac{\omega_0}{4\pi}\left[K_0 + 3g(\xi K_1 + \mu K_3)\right] \quad (27)$$

where

$$I_{b0}\left[T(x, z)\right] = I_b\left[T(x, z)\right]\frac{(1-\omega)}{(1-\omega f)}, \qquad \omega_0 = \omega\frac{(1-f)}{(1-\omega f)} \quad (28)$$

and

$$K_0 = M_0^+ + M_0^- + N_0^+ + N_0^-$$
$$K_1 = M_1^+ + M_1^- + N_1^+ + N_1^-$$
$$K_3 = M_3^+ + M_3^- + N_3^+ + N_3^- \quad (29)$$

Governing Equations

We now derive a set of moment equations from the RTE, Eq. (27), by integrating it over each domain after multiplying by 1, ξ, and μ. We thus obtain three equations for each domain. For domain 1, the RTE is written as

$$\frac{\xi}{\tau_{x0}}\frac{\partial M^+}{\partial x} + \frac{\mu}{\tau_{z0}}\frac{\partial M^+}{\partial z} + M^+$$
$$= I_{b0}(T) + \frac{\omega_0}{4\pi}\left[K_0 + 3g(\xi K_1 + \mu K_3)\right] \quad (30)$$

We multiply Eq. (30) by 1, ξ, and μ, respectively, and integrate over Ω_1 to get

$$\frac{1}{\tau_{x0}}\frac{\partial M_1^+}{\partial x} + \frac{1}{\tau_{z0}}\frac{\partial M_3^+}{\partial z} + M_0^+ = \pi I_{b0}(T)$$
$$+ \frac{\omega_0}{4\pi}\left[\pi K_0 + 3g\left(\frac{\pi}{2}K_1 + \frac{\pi}{2}K_3\right)\right] \quad (31)$$

$$\frac{1}{\tau_{x0}}\frac{\partial M_{11}^+}{\partial x} + \frac{1}{\tau_{z0}}\frac{\partial M_{13}^+}{\partial z} + M_1^+ = \frac{\pi}{2}I_{b0}(T)$$
$$+ \frac{\omega_0}{4\pi}\left[\frac{\pi}{2}K_0 + 3g\left(\frac{\pi}{3}K_1 + \frac{2}{3}K_3\right)\right] \quad (32)$$

$$\frac{1}{\tau_{x0}}\frac{\partial M_{13}^+}{\partial x} + \frac{1}{\tau_{z0}}\frac{\partial M_{33}^+}{\partial z} + M_3^+ = \frac{\pi}{2}I_{b0}(T)$$
$$+ \frac{\omega_0}{4\pi}\left[\frac{\pi}{2}K_0 + 3g\left(\frac{2}{3}K_1 + \frac{\pi}{3}K_3\right)\right] \quad (33)$$

If we use the double moment relations, Eqs. (19–21), Eqs. (31–33) can be modified as

$$\frac{1}{\tau_{x0}}\frac{\partial M_1^{\pm}}{\partial x} = \pi I_{b0} + \frac{\omega_0}{4}\left[K_0 + \frac{3g}{2}\left(K_1 \pm K_3\right)\right]$$
$$- M_0^{\pm} - \frac{1}{\tau_{z0}}\frac{\partial M_3^{\pm}}{\partial z} \quad (34)$$

$$\frac{P_1}{\tau_{x0}}\frac{\partial M_0^{\pm}}{\partial x} \pm \frac{P_4}{\tau_{z0}}\frac{\partial M_0^{\pm}}{\partial z} = \frac{\pi I_{b0}}{2} + \frac{\omega_0}{4}\left[\frac{K_0}{2} + g\left(K_1 \pm \frac{2K_3}{\pi}\right)\right]$$
$$- M_1^{\pm} - \frac{1}{\tau_{x0}}\left(P_2\frac{\partial M_1^{\pm}}{\partial x} \pm P_3\frac{\partial M_3^{\pm}}{\partial x}\right)$$
$$- \frac{P_5}{\tau_{z0}}\left(\pm\frac{\partial M_1^+}{\partial z} + \frac{\partial M_3^+}{\partial z}\right) \quad (35)$$

$$\frac{P_5}{\tau_{x0}}\frac{\partial M_3^{\pm}}{\partial x} \pm \frac{P_2}{\tau_{z0}}\frac{\partial M_3^{\pm}}{\partial z} = \frac{\pi I_{b0}}{2} + \frac{\omega_0}{4}\left[\pm\frac{K_0}{2} + g\left(\frac{\pm 2K_1}{\pi} + K_3\right)\right]$$
$$- M_3^{\pm} - \frac{1}{\tau_{x0}}\left(\pm P_4\frac{\partial M_0^{\pm}}{\partial x} \pm P_5\frac{\partial M_1^{\pm}}{\partial x}\right)$$
$$- \frac{1}{\tau_{z0}}\left(P_1\frac{\partial M_0^{\pm}}{\partial z} + P_3\frac{\partial M_1^{\pm}}{\partial z}\right) \quad (36)$$

In these equations, the upper sign is for domain 1, and the lower sign is for domain 2. Similarly, for domains 3 and 4 we obtain

$$\frac{1}{\tau_{x0}}\frac{\partial N_1^{\pm}}{\partial x} = \pi I_{b0} + \frac{\omega_0}{4}\left[K_0 + \frac{3g}{2}\left(-K_1 \pm K_3\right)\right]$$
$$- N_0^{\pm} - \frac{1}{\tau_{z0}}\frac{\partial N_3^{\pm}}{\partial z} \quad (37)$$

$$\frac{P_1}{\tau_{x0}}\frac{\partial N_0^{\pm}}{\partial x} \mp \frac{P_4}{\tau_{z0}}\frac{\partial N_0^{\pm}}{\partial z} = -\frac{\pi}{2}I_{b0} + \frac{\omega_0}{4}\left[-\frac{K_0}{2} + g\left(K_1 \mp \frac{2K_3}{\pi}\right)\right]$$
$$- N_1^{\pm} - \frac{1}{\tau_{x0}}\left(-P_2\frac{\partial N_1^{\pm}}{\partial x} \pm P_3\frac{\partial N_3^{\pm}}{\partial x}\right)$$
$$- \frac{P_5}{\tau_{z0}}\left(\pm\frac{\partial N_1^{\pm}}{\partial z} \pm \frac{\partial N_3^{\pm}}{\partial z}\right) \quad (38)$$

$$-\frac{P_5}{\tau_{x0}}\frac{\partial N_3^{\pm}}{\partial x} \pm \frac{P_2}{\tau_{z0}}\frac{\partial N_3^{\pm}}{\partial z} = \pm\frac{\pi}{2}I_{b0} + \frac{\omega_0}{4}\left[\pm\frac{K_0}{2} + g\left(\mp\frac{2K_1}{3\pi} + K_3\right)\right]$$
$$- N_3^{\pm} - \frac{1}{\tau_{x0}}\left(\mp P_4\frac{\partial N_0^+}{\partial x} \pm P_5\frac{\partial N_1^+}{\partial x}\right)$$
$$- \frac{1}{\tau_{z0}}\left(P_1\frac{\partial N_0^+}{\partial z} - P_3\frac{\partial N_1^+}{\partial z}\right) \quad (39)$$

where the upper sign is for domain 3 and the lower sign is for domain 4. Equations (34–39) constitute a system of 12 first-order differential equations in terms of the moments $M_0^{\pm}$, $N_0^{\pm}$, $M_1^{\pm}$, $N_1^{\pm}$, $M_3^{\pm}$, and $N_3^{\pm}$, and they have to be solved simultaneously subject to the boundary conditions of the physical problem. It is worthy to note that Eqs. (34) and (37) were obtained for the first-order moments in the x direction after multiplying the RTE by 1 and then integrating over the corresponding domain, Eqs. (35) and (38) were obtained for the zeroth-order moments by integrating the RTE after multiplying by ξ, and Eqs. (36) and (39) were obtained for the first-order moments in the z direction after multiplying the RTE by μ.

Boundary Conditions

The walls of the enclosure are assumed diffusely emitting and reflecting. We use Marshak's boundary equation in each domain, which is written as

$$\int_{\Omega_j} I(x, z, \Omega) l \, d\Omega_j = \int_{\Omega_j} h_w l \, d\Omega_j, \qquad j = 1, 2, 3, 4 \tag{40}$$

l takes values 1, ξ, or μ. For emitting and diffusely reflecting boundaries, the h_w function is

$$h_w(x, z, \Omega) = \epsilon_w I_b(T_w) + \frac{\rho_w^d}{\pi} \int_{\Omega' = 2\pi} I(x, z, \Omega') l_i \, d\Omega' \tag{41}$$

Here, l_i is the appropriate direction cosine ξ or μ. The variation of θ and ϕ for each boundary is shown in Table 4. We determine h_w for sides 1, 2, 3, and 4 from Eq. (41)

$$h_1 = \epsilon_1 I_b(T_1) + \frac{\rho_1^d}{\pi}(N_1^+ + N_1^-) \tag{42}$$

$$h_2 = \epsilon_2 I_b(T_2) + \frac{\rho_2^d}{\pi}(M_3^- + N_3^-) \tag{43}$$

$$h_3 = \epsilon_3 I_b(T_3) - \frac{\rho_3^d}{\pi}(M_1^+ + M_1^-) \tag{44}$$

$$h_4 = \epsilon_4 I_b(T_4) - \frac{\rho_4^d}{\pi}(M_3^+ + N_3^+) \tag{45}$$

We now substitute h_1, h_2, h_3, and h_4 into Eq. (40) and integrate over each domain to get the boundary conditions for the governing equations

Side 1

$$M_0^+ = \pi h_1, \quad M_0^- = \pi h_1, \quad M_1^+ = \frac{\pi h_1}{2}, \quad M_1^- = \frac{\pi h_1}{2},$$

$$M_3^+ = \frac{\pi h_1}{2}, \quad M_3^- = -\frac{\pi h_1}{2}$$

Table 4 Angular division for the boundary conditions, Eq. (40)

Side	θ	ϕ
1	$0/\pi$	$-\frac{\pi}{2}/\frac{\pi}{2}$
2	$0/\frac{\pi}{2}$	$0/2\pi$
3	$0/\pi$	$\frac{\pi}{2}/\frac{3\pi}{2}$
4	$\frac{\pi}{2}/\pi$	$0/2\pi$

Side 2

$$M_0^+ = \pi h_2, \quad N_0^+ = \pi h_2, \quad M_1^+ = \frac{\pi h_2}{2}, \quad N_1^+ = -\frac{\pi h_2}{2},$$

$$M_3^+ = \frac{\pi h_2}{2}, \quad N_3^+ = \frac{\pi h_2}{2}$$

Side 3

$$N_0^+ = \pi h_3, \quad N_0^- = \pi h_3, \quad N_1^+ = -\frac{\pi h_3}{2}, \quad N_1^- = -\frac{\pi h_2}{2},$$

$$N_3^+ = \frac{\pi h_3}{2}, \quad N_3^- = -\frac{\pi h_3}{2}$$

Side 4

$$M_0^- = \pi h_4, \quad N_0^- = \pi h_4, \quad M_1^- = \frac{\pi h_4}{2}, \quad N_1^- = -\frac{\pi h_4}{2},$$

$$M_3^- = -\frac{\pi h_4}{2}, \quad N_3^- = -\frac{\pi h_4}{2}$$

Radiative Heat Flux

Radiative heat fluxes in the positive and negative x directions are given as

$$q_x^+ = (M_1^+ + M_1^-), \qquad q_x^- = -(N_1^+ + N_1^-) \tag{46}$$

Net radiative heat flux in the x direction becomes

$$q_x = (M_1^+ + M_1^- + N_1^+ + N_1^-) \tag{47}$$

Radiative heat fluxes in the positive and negative z directions are expressed similarly

$$q_z^+ = (M_3^+ + N_3^+), \qquad q_z^- = -(M_3^- + N_3^-) \tag{48}$$

Again, the net radiative flux in the z direction is given as

$$q_z = (M_3^+ + M_3^- + N_3^+ + N_3^-) \tag{49}$$

Solution Method

Equations (34–39) are solved along with the boundary conditions using either any available computer code or by developing a dedicated algorithm. In this study, we used the DISPL2 code.[19] The package is capable of handling nonlinear systems of second-order partial differential equations with nonlinear boundary conditions. DISPL2 is used by specifying the number of grid points and by using a polynomial approximation between the grid points. These two parameters determine the accuracy of the solution.

In our calculations, we used a combination of eight grid points and a third-order polynomial fit. Increasing the order of the polynomial did not affect the accuracy of results at all; increasing the number of grid points increased the computation time considerably. It is, however, important to note that the required CPU time is for the simultaneous solution of 12 second-order differential equations, because DISPL2 treats a system of first-order differential equations as a system of second-order equations with appropriate zero coefficients. Consequently, the use of DISPL2 for our system of equations makes the process inefficient as far as computer time requirements are considered.

Results and Discussion

In this section, the quadruple spherical harmonics (QP_1) approximation is evaluated by comparing the results for the radiative heat flux and temperature distributions in a two-dimensional rectangular enclosure against the exact results

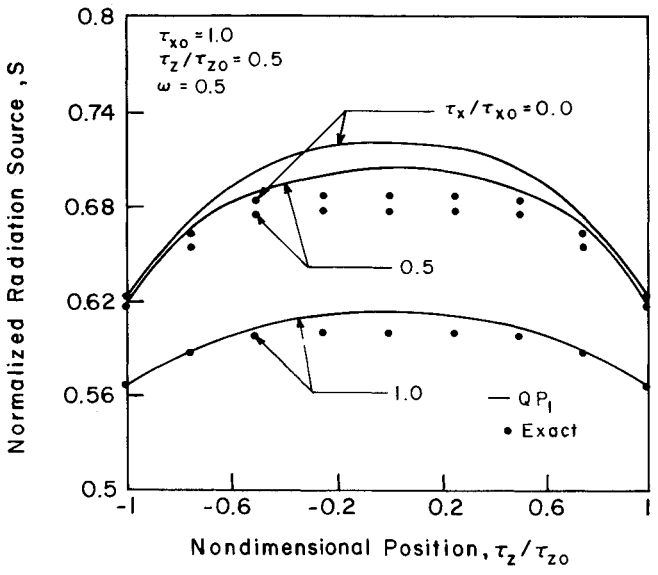

Fig. 3 Comparison of the source function $S(x, z)$ for the QP$_1$ approximation (lines) and the exact solution[20] (points).

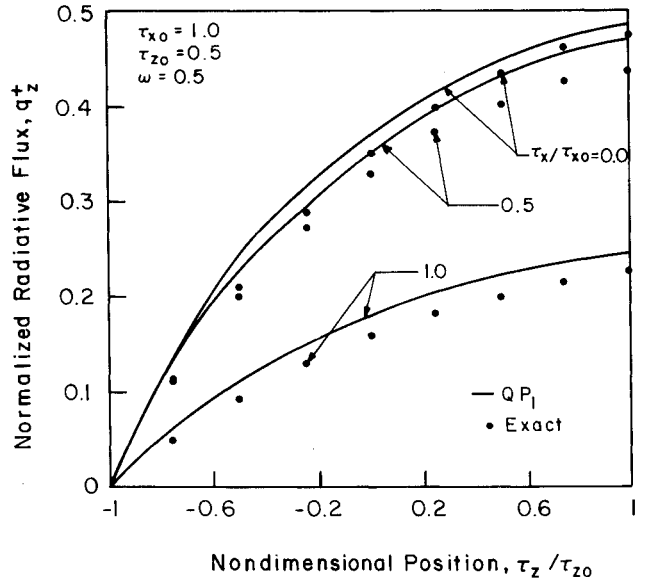

Fig. 4 Comparison of the radiative heat fluxes q_z^+ (x, z) for the QP$_1$ approximation (lines) and the exact solution[20] (points).

available in the literature. Modeling of radiation heat transfer in multidimensional geometries is much more complicated than that for one-dimensional systems. Because of this, there are only few accounts available in the literature in which the exact solutions of the RTE in two-dimensional enclosures are reported.[20-22] Here, the results from these studies will be used as the "benchmark" for comparison.

The results obtained by the QP$_1$ approximation are compared against the corresponding exact values given by Sutton and Özisik[20] in Figs. 3 and 4. The physical problem considered here is that of a rectangular enclosure, with cold boundaries and uniformly distributed source function. Isotropic phase function is considered in the analysis with $\omega = 0.5$, $\tau_{x0} = 1.0$, and $\tau_{z0} = 0.5$.

Figure 3 shows the plot of the source function $S(x, z)$ against the optical distance z at three x locations. The agreement between the exact[20] and the QP$_1$ approximation results is very good as the error is always less than 5% at all locations. The maximum error is in the central region of the

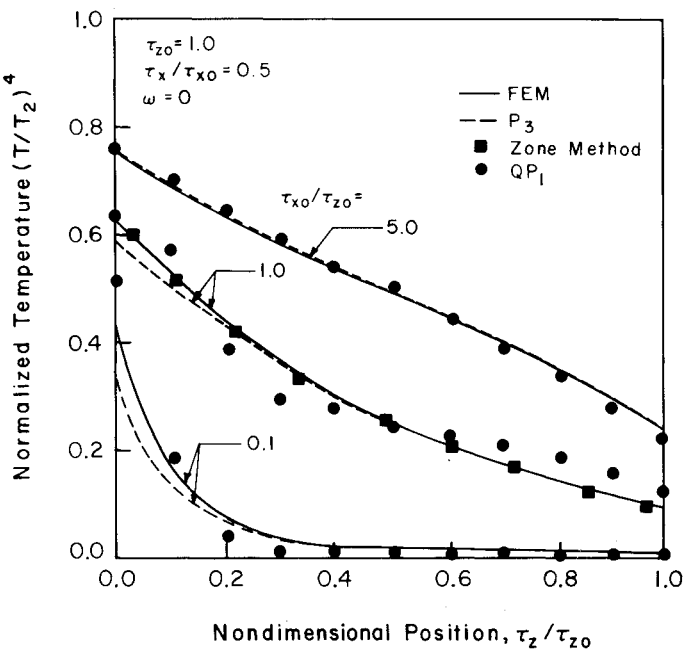

Fig. 5 Nondimensional centerline temperature profiles in rectangular enclosures of different aspect ratios. Zonal and FEM methods are from Razzaque et al.,[21] P$_3$ approximation from Ratzel and Howell.[23] [$I_b(T_2) = 1.0$; $I_b(T_i) = 0$; $i = 1, 3, 4$; $\omega = 0$; $\epsilon_i = 1.0$.]

rectangular enclosure and decreases toward the sides. Figure 4 depicts the distribution of radiative heat flux components q_z^+ (or $1 - q_z^-$) along the z axis. The results are in good agreement with the exact values as the maximum error is less than 10%. Note that because of the symmetry, q_z^+ and q_z^- are mirror images of each other.

The effect of the aspect ratios of the rectangular enclosure on the temperatures and heat flux predictions is discussed next. For these calculations, the results of the Hottel's zonal and the finite-element model (FEM) as reported by Razzaque et al.[21] serve as the benchmark for comparison. Also, the P$_3$ approximation results, as given by Ratzel and Howell,[23] are compared against the QP$_1$ approximation. In the physical model, it is assumed that surface 2 ($x = 0$) is at a nondimensional temperature of unity, whereas the other walls are cold. All the walls are considered black. Figure 5 shows the nondimensional centerline temperatures plotted against the optical distance in the z direction for aspect ratios (τ_{x0}/τ_{z0}) of 0.1, 1.0, and 5.0. The agreement between the QP$_1$ approximation and the finite-element and zone method solutions for different aspect ratios is good. It is important to note that the agreement for (T/T_2) is much better than that presented for $(T/T_2)^4$. The effect of aspect ratio on the radiative heat flux at the lower boundary is depicted in Fig. 6. Again, the agreement between the QP$_1$ approximation and finite-element solutions is excellent, and it is better than that for the P$_3$ approximation.[23] These results would indicate that the aspect ratio has little influence on the accuracy of the QP$_1$ approximation predictions.

The effect of optical thickness on the heat flux distribution in square enclosures is shown in Fig. 7. The lower boundary surface ($x = 0$) is maintained at a nondimensional temperature of unity and the other boundary surfaces are assumed cold. The system is in radiative equilibrium and nonscattering ($\omega = 0$). Three different optical thicknesses of 0.1, 1.0, and 2.0 are considered. From the figure, it is seen that the heat flux predictions obtained using the QP$_1$ approximation are in very good agreement with the benchmark solutions in which the P$_3$ approximation shows substantial error especially for low optical thicknesses. Although the evaluation of the QP$_1$ approximation was given for a limited range of optical

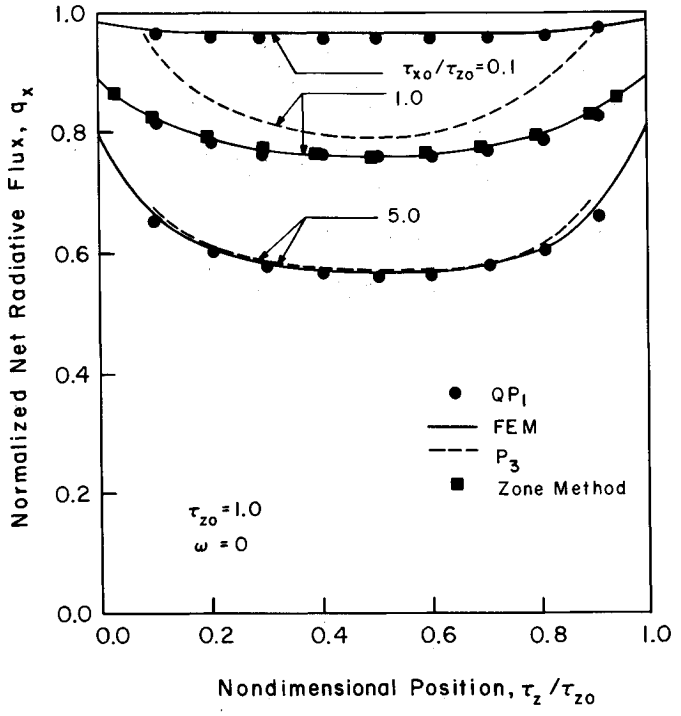

Fig. 6 Nondimensional net radiative flux at $x = 0$ in rectangular enclosures of different aspect ratios. Zonal and FEM methods are from Razzaque et al.,[21] P_3 approximation from Ratzel and Howell.[23] [$I_b(T_2) = 1.0$; $I_b(T_i) = 0$; $i = 1, 3, 4$; $\omega = 0$; $\epsilon_i = 1.0$.]

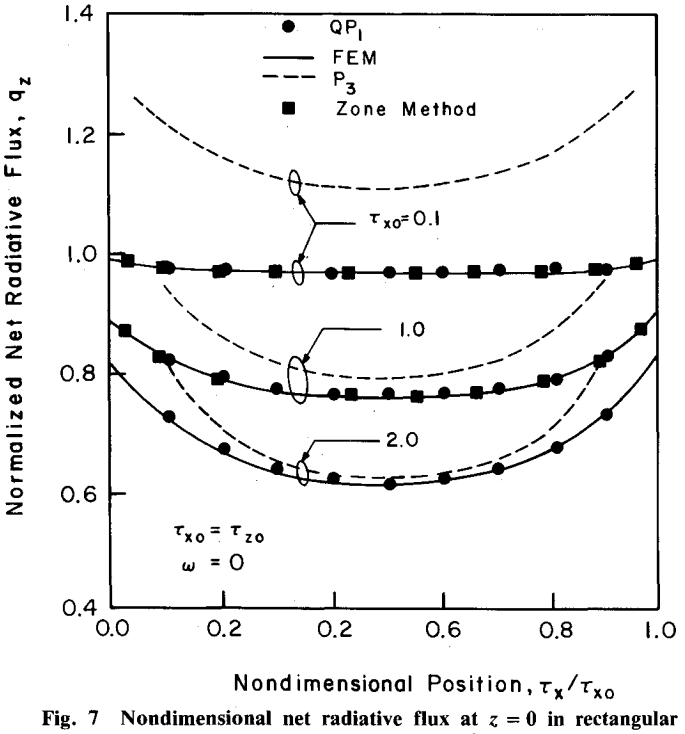

Fig. 7 Nondimensional net radiative flux at $z = 0$ in rectangular enclosures of different optical thicknesses. Zonal and FEM methods are from Razzaque et al.,[21] P_3 approximation from Ratzel and Howell.[23] [$I_b(T_2) = 1.0$; $I_b(T_i) = 0$; $i = 1, 3, 4$; $\omega = 0$; $\epsilon_i = 1.0$.]

thicknesses, it is expected to have good accuracy also at larger τ values, as observed for the DP_1 approximation.[15]

The effect of optical thickness on the temperature distributions is shown in Fig. 8 for the same problem just described for $\tau_{x0} = \tau_{z0} = 1$. Similar trends of results are also observed for optical thicknesses of 0.1 and 2.0. Note again that the results are presented for $(T/T_2)^4$; the percent error for the absolute temperature T is much smaller than that shown in these figures.

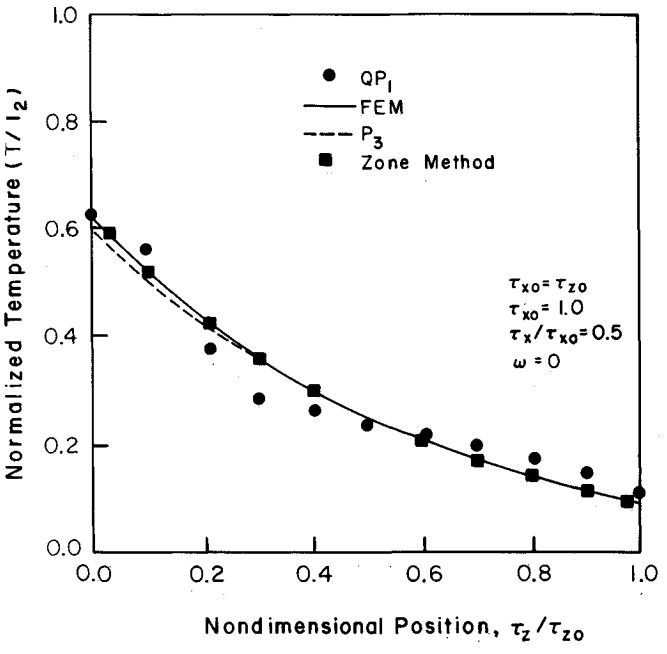

Fig. 8 Nondimensional centerline temperature profiles in rectangular enclosures of different aspect ratios. Zonal and FEM methods are from Razzaque et al.,[21] P_3 approximation from Ratzel and Howell.[23] [$I_b(T_2) = 1.0$; $I_b(T_i) = 0$; $i = 1, 3, 4$; $\omega = 0$; $\epsilon_i = 1.0$.]

Although it is also desirable to discuss the effects of other parameters, such as wall temperature, wall emissivity, scattering phase function as well as the nonuniform property distributions in the medium, because of the space constraints and lack of benchmark results to evaluate the model, these effects are not discussed in this paper.

Conclusions

In this paper, a hybrid model has been introduced for the solution of the radiative transfer equation in two-dimensional, rectangular enclosures. The QP_1 approximation combines the attractive features of the flux approach and spherical harmonics approximation. The governing equations of the present model are the first-order, ordinary differential equations, which can be solved easily. This is the main advantage of the method. The algebra needed to set up the equations, however, is much more complicated than that required for the flux methods. Because the derivation of the governing equations is to be worked out only once, this does not seem to be a serious drawback of the model.

The proposed model has been evaluated against two different "exact" techniques. In general, the QP_1 approximation predictions of the radiative flux distribution agreed very well with the benchmark results obtained from the exact models. The agreement for the temperature distributions, however, was not so good.

The DISPL2 code used in solving the governing equations of the QP_1 method is one of the major sources of error. This code is designed specifically for the second-order differential equations; thus, it was inefficient for our problem. The use of spline fit is reflected in the results, which display oscillatory behavior around the true values. The accuracy of the QP_1 approximation can be improved significantly if a dedicated computer algorithm is written to solve the corresponding first-order differential equations simultaneously. This would increase the speed of the solution and allow the user to adapt a finer grid scheme, which would increase the accuracy of the model further.

An extension of this model can be obtained by increasing the number of subdivisions. For example, if the radiation field

is very strongly anisotropic near the boundaries, then the solid angle is to be divided into finer subangles. This would improve the accuracy of the predictions; however, the model will be more tedious to set up and the computational time needed will be more.

Appendix: Constants of the QP_1 Approximation

$$G = \frac{\pi^3}{9}\left(1-\frac{2}{\pi}\right)\left(\frac{2}{\pi}-\frac{1}{2}\right)$$

$$a_1 = \frac{\pi^2}{9G}\left(1-\frac{4}{\pi^2}\right)$$

$$a_2 = -\frac{\pi^2}{6G}\left(1-\frac{2}{\pi}\right)$$

$$a_3 = \frac{\pi^2}{12G}$$

$$a_4 = \frac{\pi^2}{G}\left(\frac{1}{4}-\frac{2}{3\pi}\right)$$

$$P_1 = \pi\left(\frac{a_1}{3}+\frac{3a_2}{8}\right)$$

$$P_2 = \pi\left(\frac{a_2}{3}+\frac{a_3}{4}+\frac{a_4}{8}\right)$$

$$P_3 = \pi\left(\frac{a_2}{3}+\frac{a_3}{8}+\frac{a_4}{4}\right)$$

$$P_4 = \pi\left(\frac{2a_1}{3\pi}+\frac{a_2}{4}\right)$$

$$P_5 = \pi\left(\frac{2a_2}{3\pi}+\frac{a_3}{8}+\frac{a_4}{8}\right)$$

Acknowledgments

This work was partially supported by the NSF-EPSCoR Computational Sciences Project at the University of Kentucky. Also, the University of Kentucky Summer Faculty Research Fellowship to M. P. Mengüc is gratefully acknowledged.

References

[1]Viskanta, R. and Mengüc M. P., "Radiation Heat Transfer in Combustion Systems," *Progress in Energy and Combustion Sciences,* Vol. 13, No. 2, 1987, pp. 97–160.

[2]Viskanta, R., "Radiative Heat Transfer," *Fortschritte de Verfahrenstechnik,* Vol. 22, Section A, 1984, pp. 51–81.

[3]Viskanta, R. and Mengüc M. P., "Modeling of Radiative Heat Transfer," *Library of Environmental Technology* (to be published) 1988.

[4]Krook, M., "On the Solution of Equations of Transfer. I," *Astrophysics Journal,* Vol. 122, 1955, pp. 488–497.

[5]Yvon, J., "La Diffusion Macroscopique des Neutrons une Methode D'approximation," *Journal of Nuclear Energy,* Vol. 4, 1957, pp. 305–318.

[6]Ziering, S. and Schiff, D., "Yvon's Method for Slabs," *Nuclear Science and Engineering,* Vol. 3, 1958, pp. 635–647.

[7]Schiff, D. and Ziering, S., "Many-Fold Moment Method," *Nuclear Science and Engineering,* Vol. 7, 1960, pp. 172–183.

[8]Le Sage, L. G., "Application of the Double Spherical Harmonics Method to the One-Dimensional Radiation-Transfer Equation," NASA TN D-2589, 1965.

[9]Özisik, M. N., Menning, J., and Halg, W., "Half-Range Moment Method for Solution of the Transport Equation in a Spherically Symmetric Geometry," *Journal of Quantitative Spectroscopy and Radiative Transfer,* Vol. 15, 1975, pp. 1101–1106.

[10]Sherman, M. P., "Moment Methods in Radiative Transfer Problems," *Journal of Quantitative Spectroscopy and Radiative Transfer,* Vol. 7, 1967, pp. 89–109.

[11]Selçuk, N. and Siddall, R. G., "Two-Flux Spherical Harmonics Modeling of Two-Dimensional Radiative Transfer in Furnaces," *International Journal of Heat and Mass Transfer,* Vol. 19, 1976, pp. 313–321.

[12]Wan, F. S., Wilson, S. J., and Sen, K. K., "Radiative Transfer in an Isothermal Slab with Anisotropic Scattering," *Journal of Quantitative Spectroscopy and Radiative Transfer,* Vol. 17, 1977, pp. 571–575.

[13]Wilson, S. J. and Sen, K. K., "Generalized Eddington Approximation Transfer Problems in Slab Medium," *Journal of Quantitative Spectroscopy and Radiative Transfer,* Vol. 35, No. 6, 1986, pp. 467–472.

[14]Harshvardhan, Weinman, J. A., and Davies, R., "Transport of Infrared Radiation in Cuboidal Clouds," NASA TM 82116, 1981.

[15]Mengüc, M. P. and Iyer, R. K., "Modeling of Radiative Transfer Using Multiple Spherical Harmonics Approximation," *Journal of Quantitative Spectroscopy and Radiative Transfer,* Vol. 39, No. 6, 1988, pp. 445–461.

[16]Case, K. M. and Zweifel, P. F., *Linear Transport Theory,* Addison-Wesley, Reading, MA, 1967.

[17]Joseph, J. H., Wiscombe, W. J., and Weinman, J. A., "The Delta-Eddington Approximation for Radiative Heat Transfer," *Journal of Atmospheric Sciences,* Vol. 33, 1976, pp. 2452–2459.

[18]Crosbie, A. L. and Davidson, G. W., "Dirac-Delta Function Approximations to the Scattering Phase Function," *Journal of Quantitative Spectroscopy and Radiative Transfer,* Vol. 33, No. 4, 1985, pp. 391–409.

[19]Leaf, G. K. and Minkoff, M., "DISPL2—A Software Package for One and Two Spatially Dimensioned Kinetics-Diffusion Problems," Argonne Nat. Lab., Argonne, IL, ANL-84-56, 1984.

[20]Sutton, W. H. and Özisik, M. N., "An Alternative Formulation for Radiative Transfer in an Isotropically Scattering Two-Dimensional Bar Geometry and Solution Using the Source Function Expansion Method," American Society of Mechanical Engineers, Paper 84-HT-36, 1984.

[21]Razzaque, M. M., Klein, D. E., and Howell, J. R., "Finite Element Solution of Radiative Heat Transfer in Two-Dimensional Rectangular Enclosure with Gray Participating Media," ASME Paper 82-WA/HT-51, 1982; for a shortened revision, see also *Journal of Heat Transfer,* Vol. 105, 1983, pp. 933–936.

[22]Crosbie, A. L. and Schrenker, R. G., "Radiative Transfer in a Two-Dimensional Rectangular Medium Exposed to Diffuse Radiation," *Journal of Quantitative Spectroscopy and Radiative Transfer,* Vol. 28, 1984, pp. 339–372.

[23]Ratzel, A. C., III and Howell, J. R., "Two Dimensional Radiation in Absorbing-Emitting Media Using the P_N-Approximation," *Journal of Heat Transfer,* Vol. 105, 1983, pp. 333–340.